# ESTIMATION OF THE ELECTRODES SPUTTERING OF THE MINIATURE LINER ACCELERATOR

I.A. Kanshin[1], N.V. Mamedov[1,2], A.A. Solodovnikov[1], N.E. Efimov[2]

[1] Dukhov Automatics Research Institute (VNIIA), 22 Suschevskaya Ul., Moscow, Russia,127055,
[2] National Research Nuclear University MEPhI, Kashirskoest., 31, Moscow, Russia, 115409.

VNIIA ROSATOM

Ion-Surface Interactions 2021

XXV

## I. Introduction

**Miniature linear accelerators (MLA**) are widely applied in many science and technology fields, such as, in a **sealed neutron generator**, which can be used in oil well logging, neutron activation analysis, explosive detection, coal analysis [1,2]. **D + T → α(3.5 MeV) + n(14.1 MeV).**

One of the main reasons for failure work MLA is the decrease electrical strength of the high-voltage insulator. It is often associated with a change in the surface conductivity of the high-voltage insulator due to deposition on its inner surface metal layer during prolonged operation. When a certain thickness of the conductive metal layer is formed on the insulator between the accelerating electrode and the focusing electrodes, a high-voltage breakdown is provoked [3]. The metal layer is under a floating potential and is gradually charged, so its potential increases. There is a distortion of the initial potential distribution. And when the maximum field strength is reached, a breakdown occurs along the surface of the insulator. If this process is repeated repeatedly, the MLA will stop working [3,4].

Before work

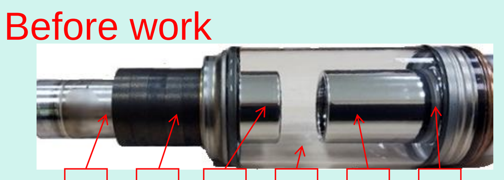


**MLA general view.**
1 - Penning ion source,
2 – Magnets,
3 - Focusing electrode,
4 - High-voltage insulator,
5 - Accelerating electrode,
6 - Neutron-forming target.


Breakdown

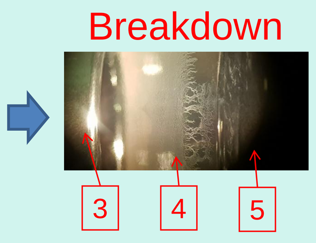


Distributions of the deposition layer (intensity of darkening on the insulator surface) obtained during digitization of the image using the Image J program

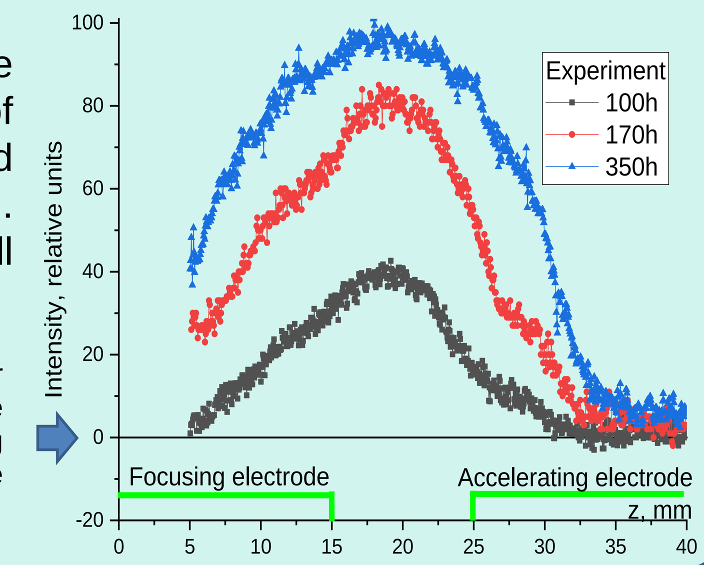


## II. Trajectory analysis of corpuscular flows in MLA by Comsol simulations

To determine the electrode sputtering areas, it is necessary to consider additional processes of interaction of the ion beam with the residual gas during its transportation to the MLA.
The simulation took into account the resonant recharge $H_2^+ + H_2^0 = H_2^0 + H_2^+$ and $H_2^+ + H_2^0 = 2H_1^0 + H_2^+$

**Experimental determination of the initial parameters of the beam.**
At the initial stage, the emittance was experimentally determined, the calculation method is described in [3]. The emittance was determined in the output aperture plane of the focusing electrode [5]. Also, to form the input data for trajectory simulation, experimental results of measuring the energy spectra of the extracted ions [7] and measuring the beam profile on the target depending on the accelerating voltage were used [8].

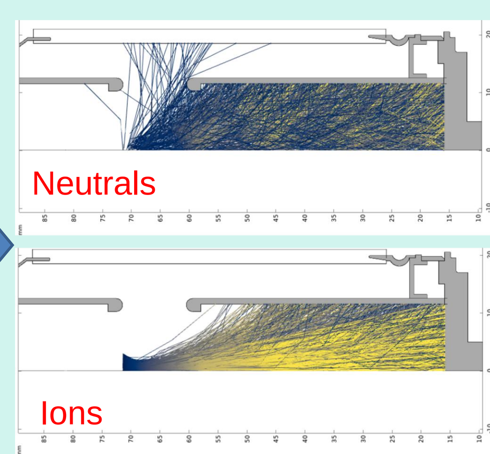


**Trajectory analysis based on the PIC data**
Since the simulation particle beam motion, based on data from [3,5], does not take into account the motion of particles in the focusing electrode, the data of Particle – in – cell (PIC) simulations of the Penning ion source were taken [12,13]. From the PIC data array particles located near the extraction aperture of ion source were selected (their position x,y,z, speed $v_x$, $v_y$, $v_z$ were recorded). After that, the sorted array of particles (approximately $50{\cdot}10^3$ particles) was loaded into COMSOL Multiphysics.

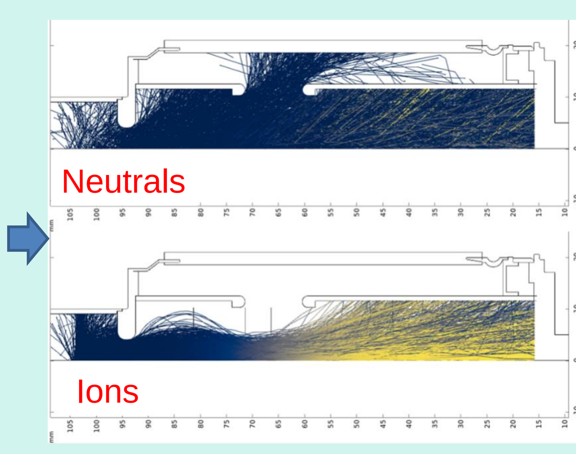


Conditional division of the surfaces of the focusing and accelerating electrodes into zones

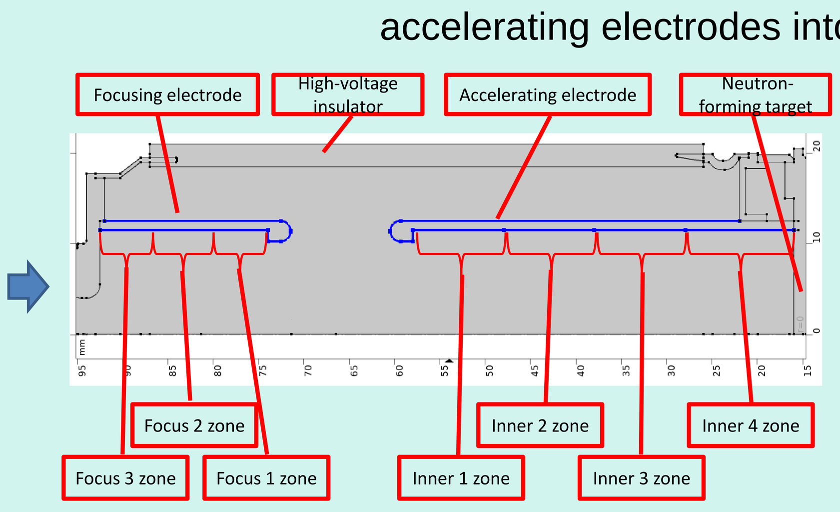


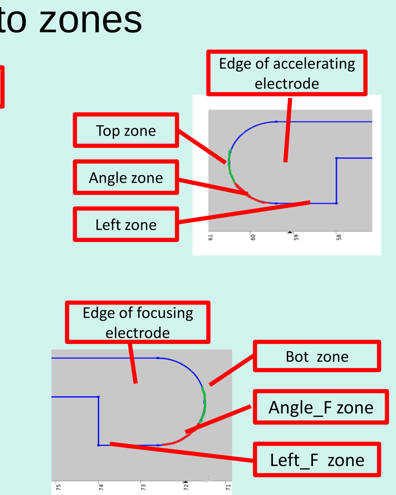


## III. Angular (above) and energy (below) distributions of charge neutrals (N) and scattered ions (I) incident on the accelerating and focusing electrodes.

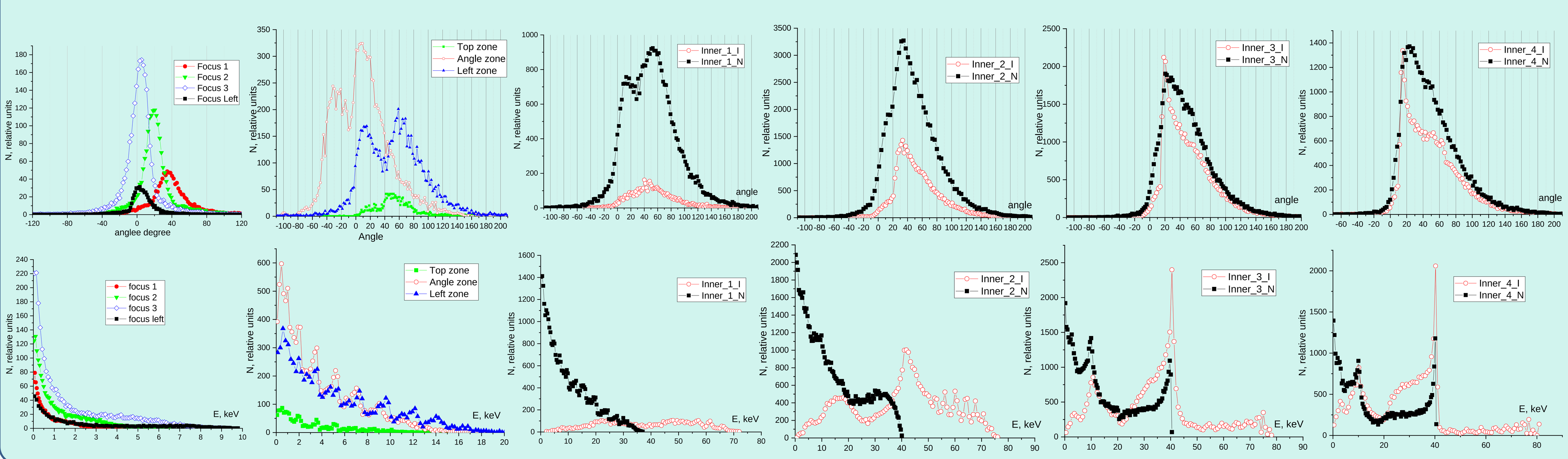


**Averaged characteristics of corpuscular flows incident on various surfaces of the focusing and accelerating electrodes.**

In the first approximation, it is possible to distinguish the characteristic angles and the average energy of the particles bombarding the surface of the electrodes by analyzed obtained angular and energy distributions.
For example,
On average, neutral particles fall into the upper zone of the accelerating electrode edge "Zone TOP" at an angle of incidence of $\Theta_0$=50° relative to the normal, with an average energy of <E> = 3 keV, 0.17% of the primary particles number incident into this electrode area.

### Initial data to BCA codes

| Electrode zone | Averaged particle characteristics: Incidence angle relative to the normal $\Theta_0$ | Averaged particle characteristics: Average particle energy, keV | Percentage % of the number of primary particles: «Emittance» data | Percentage % of the number of primary particles: PIC data |
|---|---|---|---|---|
| **Top_N** | 50° | 3 | 0,17 | 1,35 |
| **Angle_N** | -30° | 3,8 | 1,18 | 4,02 |
| | 10° | 3,8 | | |
| **Left_N** | 60° | 5,2 | 0,83 | 1,72 |
| | 15° | 5,2 | | |
| **Inner_1_ION** | 50° | 38 | 0,6 | 0,59 |
| **Inner_1_Neutral** | 10° | 10 | 3,68 | 4,42 |
| | 50° | 10 | | |
| **Inner_2_ION** | 10° | 39 | 3,52 | 3,03 |
| | 30° | 39 | | |
| **Inner_2_Neutral** | 10° | 14 | 7,37 | 7,26 |
| | 30° | 14 | | |
| **Inner_3_ION** | 20° | 33 | 4,04 | 2,7 |
| | 60° | 33 | | |
| **Inner_3_Neutral** | 20° | 16 | 6,7 | 6,47 |
| | 60° | 16 | | |
| **Inner_4_ION** | 15° | 29 | 4,04 | 2,08 |
| | 50° | 29 | | |
| **Inner_4_Neutral** | 20 ° | 17 | 4,15 | 4,8 |
| | 50° | 17 | | |
| **Σ** | | | **36,3** | **38,4** |
| **Focus_1_N** | 35° | 0,1 | - | 1,9 |
| **Focus_2_N** | 20° | 0,2 | - | 5,6 |
| **Focus_3_N** | 3° | 0,45 | - | 7,1 |
| **Focus_Left_N** | 3° | 0,13 | - | 0,5 |
| **Σ** | | | | **15,1** |
| **ΣΣ** | | | | **53,5** |

## IV. Estimation of the conductive layer deposition area on the MLA insulator

To estimate of the conductive layer deposition area on the MLA insulator , a simulations of the sputtering of the stainless steel surface (electrode material) with deuterium atoms in the BCA codes SRIM [14] and SDTrimSP [15], SCATTER [16,17], were done. The result of simulation in these BCA codes were the energy and angular spectra of reflected and sputtered particles from a small surface element. That is, the final file of the SCATTER, SRIM or SDTrimSP programs contains an array of data in which there is information about the type of particle (primary reflected from the surface or sprayed particle), its energy during departure and the direction of its leave from the surface. At the same time, the initial angular and energy distributions of incident deuterium ions and neutrals obtained as a result of trajectory analysis in COMSOL were taken into account for each electrode region. The data obtained during the sputtering simulation were loaded "back" into COMSOL Multiphysics to calculate the motion of sputtered and reflected particles in the MLA. To take into account the size (area) of the sputtered surface, the initial position of the particle was set randomly within this zone.

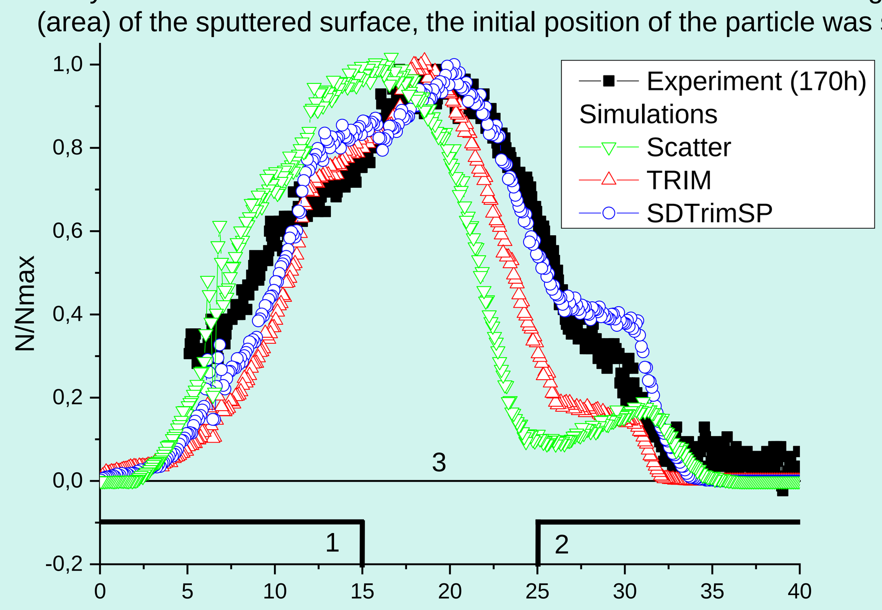


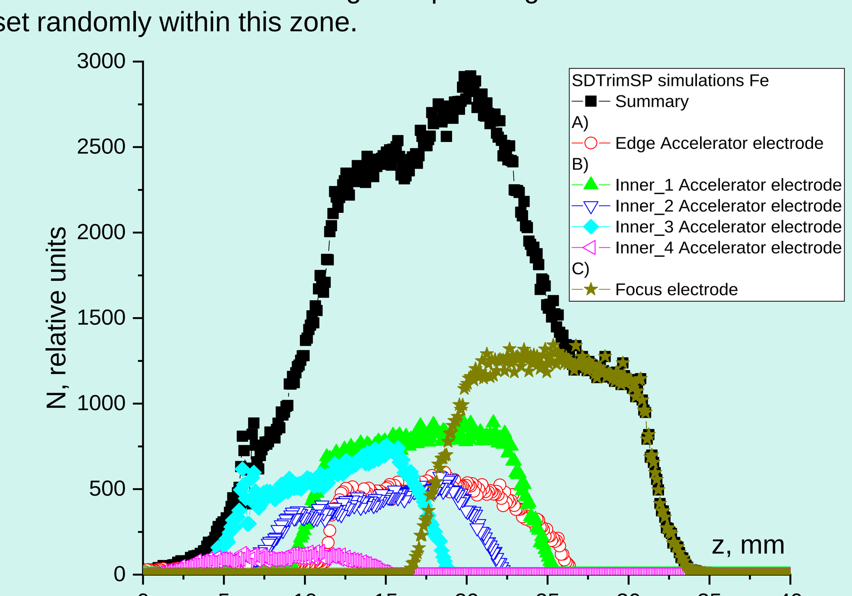


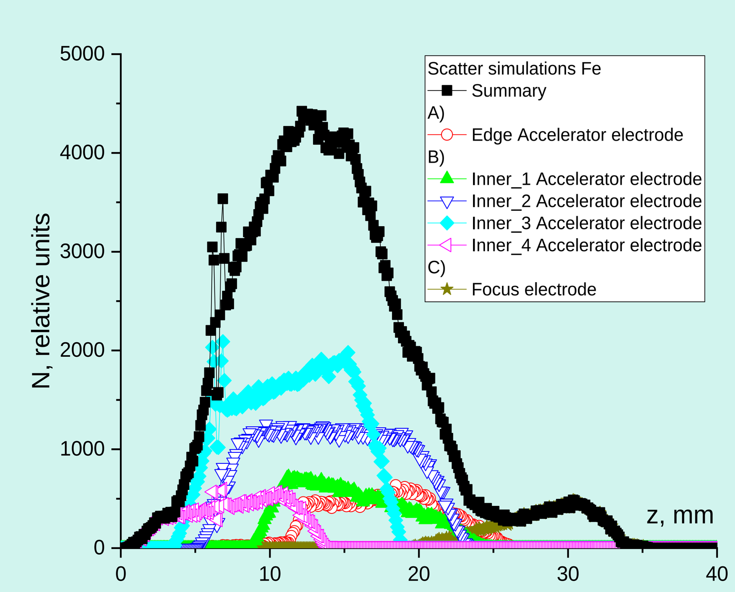


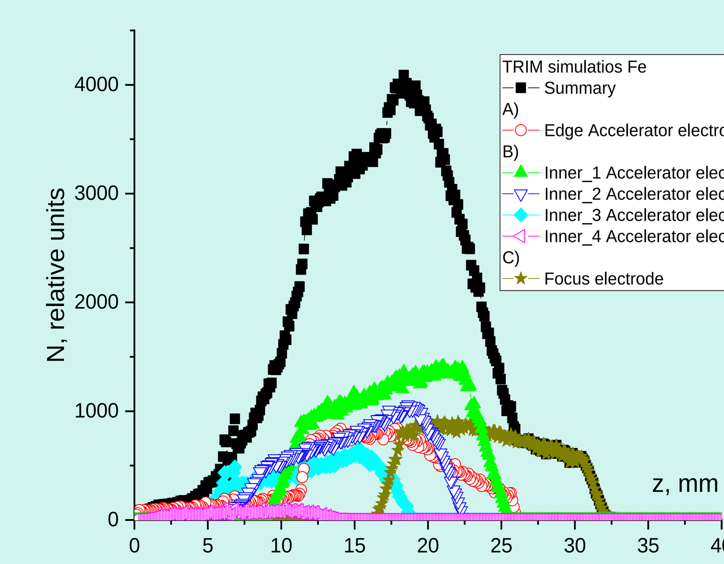


The experimental data and the simulated distribution coincide well – the total area of the sprayed layer is precisely determined. However, the maximum of the distribution of sprayed particles modeled in SCATTER is more strongly shifted to the area behind the focusing electrode, while the maxima of SRIM or SDTrimSP coincide well with the experiment. It should be noted that the results of modeling in SDTrimSP better match the experimental data. The width at the half-height of the spectrum (FWHM) for SDTrimSP coincides with the experimental one, while the FWHM for SCATTER is wider, and the FWHM for SRIM is narrower. Nevertheless, the simulated distributions , as well as the experiment, have three pronounced peaks. Figures shows the areas of sputtering of particles deposited from the edge of the accelerating electrode (a), the inner surface of the accelerating electrode (b) and the focusing electrode (c).

## V. Results SDTrimSP simulations - the distribution of Fe atoms deposited on the high-voltage insulator, sputtered from different zones of the accelerating and focusing electrode.

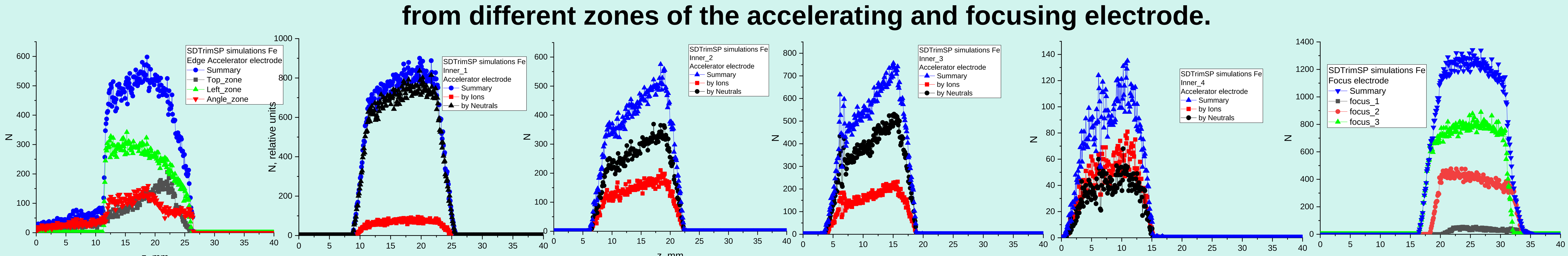


## VI. Estimation of the thickness of the deposited layer and its growth rate

Also estimates of the deposited layer thickness of and its growth rate were done. The number of Fe atoms in the layer is equal to: $n_{Fe} = 8{,}5 \cdot 10^{15}\, particle/cm^2 \cdot nm$

Thus, the deposited area on the inner insulator surface is ~23.2 cm² (with a radius of 20mm). That is, it is necessary particles to create a uniform metal layer of one nm. $n_{Fe} \cdot S \approx 2 \cdot 10^{17}\, particle/nm$

Taking into account the sputtering coefficient (based on SDTrimSP simulations) and geometric factors (based on COMSOL simulations), the sputtering coefficient (i.e., the ratio of metal particles deposited on the insulator to the particle flow to the electrodes) is equal to - $\alpha_{Fe} = 1.5 \cdot 10^{-1}$

There is 50% of the equivalent current of the main beam On the electrode surfaces. With this in mind, at an average MLA current of 100mkA, the internal surfaces of the electrodes fall: $I/e = 3.1 \cdot 10^{14}\, particle/s$

In total, we obtain that $n = I \cdot \alpha_{Fe}/e = 4.7 \cdot 10^{13}\, particle/s$ are deposited on the insulator.

Therefore, the growth rate of the metal film on the insulator can be estimated as:

$$\rho = \frac{I \cdot \alpha_{Fe}}{e \cdot n_{Fe} \cdot S} = \frac{4.7 \cdot 10^{13}\ particle/s}{2 \cdot 10^{17}\, particle/nm} = 2{,}35 \cdot 10^{-4} n\, m/s$$

$$\rho = 0.85\ nm/hour$$

This value indicates that in 100 hours the thickness of the sprayed layer will be 85 nm.

## VII. Summary

1. At a pressure of 5 mTorr, more than 35% of the particles (charge exchange neutral particles and scattered ions) from the initial beam incident on the accelerating electrode and about 15% incident on the focusing electrode. Thus, the total flow on the electrodes surfaces is about 50% of the equivalent current of the main beam incident on the target,
2. The deposited layer on the insulator is formed from three characteristic areas. In particular, particles sputtered from the edge of the accelerating electrode are deposited into the area between the focusing and accelerating electrode (10 < z < 25mm). The area of the inner accelerating electrode surface nearest to the edge deposited on the insulator of 10 < z < 25mm. The middle of the inner accelerating electrode surface is responsible for the deposition of the layer in 5 < z < 20mm. The area of the inner accelerating electrode surface located near the target forms a deposited layer in 0 < z < 15mm,
3. In the central insulator region (the interelectrode space of 15 < z < 25mm) deposited layer is a superposition from sputtering of the edge and the middle of the inner surface of the accelerating electrode ,
4. Sputtering the inner surface of the focusing electrode leads to the formation of deposition layer behind the accelerating electrode (15 < z < 35 mm),
5. Estimated value of the deposited metal layer on the insulator MLA $\rho = 0.85\ nm/hour$

V. Vladivoj, *14 MeV Neutrons. Physics and Applications*, CRC Press Taylor & Francis Group, New York (2016),
*Neutron Generators for Analytical Purposes In IAEA Radiation Technology* Reports No. 1. Vienna: International Atomic Energy Agency, 2012. 145 pp. ISBN 978-92-0-125110-7,
I.A. Kanshin and A.A. Solodovnikov // Instruments and Experimental Techniques, 2020, Vol. 63, No. 3, pp. 315–324,
*Gas sealed – neutron tube*byButolin S.L., Chermenskij V.G., Khasaev T.O. Russian patent №2451433 C1, patent pending № 2011119241/07/28 from16.05.2011,
I.A. Kanshin // Proceeding of 7th International Congress on Energy Fluxes and Radiation Effects (EFRE). 978-1-7281-2685-2/20/$31.00 2020. IEEE. DOI: 10.1109/EFRE47760.2020.9241976. pp. 474-478,
V.I. Rashchikov / Physics Procedia 74 ( 2015 ) 97 – 103, doi: 10.1016/j.phpro.2015.09.228,
N.V. Mamedov, D.V.Kolodko, I.A. Sorokin, I.A.Kanshin and D.N.Sinelnikov, IOP Conf. Series: J. Physics Conf. Series. vol. 830, p. 012063, 2017, https://doi.org/10.1088/1742-6596/830/1/012063,
N.V. Mamedov, D.E. Prokhorovich, D.I. Yurkov, I.A. Kanshin, A.A. Solodovnikov, D.V. Kolodko, and I.A. Sorokin, Instruments and Experimental Techniques., vol. 61, no. 4, pp. 530–537, 2018, DOI: 10.1134/S0020441218030223,
N.V.Mamedov, A.V.Gubarev, et al, Plasma Sources Sci. Technol. (2020), https://doi.org/10.1088/1361-6595/ab6758,
Болдасов В.С., Денбновецкий С.В., Кузьмичёв А.И. *Моделирование газоразрядных* коммутирующих приборов низкого давления. Электрическая прочность приборов в предразрядный период. – Киев ИСИО, 1996.- 140 с,
H. Tawara, Y. Itikawa, H. Nishimura et al / Journal of Physical and Chemical Reference Data. 1990. T. 19, № 3. p. 617–636.
N.V. Mamedov, A. S. Rohmanenkov, et al, Rev. Sci. Instrum. 90, 123310 (2019), doi: 10.1063/1.5127921
A.S. Rokhmanenkov , S.E. Kuratov, IOP Conf. Series: Journal of Physics: Conf. Series 1250 (2019) 012036 doi:10.1088/1742-6596/1250/1/012036
www.srim.org
Eckstein, W., Dohmen, R., Mutzke, A., & Schneider, R. (2007). *SDTrimSP: Ein Monte-Carlo Code zurBerechnung von Stossereignissen in ungeordneten Targets = SDTrimSP: A Monte-Carlo Code for Calculating Collision Phenomena in Randomized Targets* (IPP 12/3). Garching: Max-Planck-InstitutfürPlasmaphysik.
V.A. Kurnaev, Trifonov N.N., Drozdov M.N., Salashchenko N.N. // Vacuum 56, (2000), p. 253-255, doi.org/10.1016/S0042-207X(00)00136-6
N.N.Trifonov, Interaction of hydrogen ions of thermonuclear energies with thin layers of matter, Cand. Sci. (Phys.–Math.) Dissertation, Moscow: Natl. Res. Nucl. Univ.MEPhI, 2002 (in Russian).
H. Hofsass, K. Zhang, A. Mutzke, Applied Surface Science 314 (2014), 134-141, doi.org/10.1016/j.apsusc.2014.03.152
R. Arredondo et al. Nuclear Materials and Energy 18 (2019) 72–76, doi.org/10.1016/j.nme.2018.12.007